



Article

Application of Grasshopper Optimization Algorithm for Selective Harmonics Elimination in Low-Frequency Voltage Source Inverter

Marcin Steczek * , Włodzimierz Jefimowski and Adam Szlag 

Faculty of Electrical Engineering, Institute of Electrical Power Engineering, Warsaw University of Technology, pl. Politechniki 1, 00-661 Warszawa, Poland; wlodzimierz.jefimowski@ien.pw.edu.pl (W.J.); adam.szlag@ien.pw.edu.pl (A.S.)

* Correspondence: marcin.steczek@ien.pw.edu.pl

Received: 28 October 2020; Accepted: 2 December 2020; Published: 4 December 2020



Abstract: In this paper, an application of the recently developed Grasshopper Optimization Algorithm (GOA) for calculation of switching angles for Selective Harmonic Elimination (SHE) PWM in low-frequency voltage source inverter is proposed. The algorithm is based on insect behavior in the food foraging swarm of grasshoppers. The characteristic feature of GOA is the movement of agents is based on the position of all agents in the swarm. This method represents a higher probability of convergence than Particle Swarm Optimization (PSO) Modifications of GOA have been examined regarding their effect on the algorithm's convergence. The proposed modifications were based on the following techniques: Grey Wolf Optimizer (GWO), Natural Selection (NS), Adaptive Grasshopper Optimization Algorithm (AGOA), and Opposite Based Learning (OBL). The performance of GOA and its modifications were compared with well-known PSO. Areas, where GOA is superior to PSO in terms of probability of convergence, have been shown. The efficiency of the GOA algorithm applied for solving the SHE problem was confirmed by measurements in the laboratory.

Keywords: grasshopper optimization algorithm (GOA); particle swarm optimization (PSO); voltage source inverter (VSI); selective harmonics elimination PWM (SHEPWM)

1. Introduction

The Selective Harmonic Elimination (SHE) and Selective Harmonic Mitigation (SHM) [1,2] has been described for the first time in the 1960s in [3] and disseminated by Patel and Hoft [4,5]. Since that time SHE has been introduced in a number of industrial applications where power electronics was proposed [6]. The challenge is progress in the development of techniques for solving SHE/SHM non-linear transcendental equations

Since the early days, iterative techniques such as Newton–Raphson (N–R) [4,5], Gauss–Newton have been employed to solve these equations. The convergence of these methods depends on the initial guess, which is a complex problem and in many cases is not successful. This disadvantage encourages researchers to develop more effective techniques. Thus, Chaison et al. in [7] proposed the method based on the conversion of transcendental equations into an equivalent set of polynomials. The high degree of polynomial requires specialized software to compute it. The combination of Groebner's bases and symmetric polynomials was applied to solve the mentioned polynomials [8]. However, it generates ambiguous solutions which make it less useful. The main disadvantage of iterative techniques is they do not find an optimum solution.

The development of evolutionary algorithms opens new opportunities in the field of solving SHE equations [9]. These algorithms present numerous benefits such as independence from an initial guess,

utilization of simple algebra, lower computational costs, formulation of multi-constrained problems. One of the most popular evolutionary algorithms is Particle Swarm Optimization (PSO) proposed for finding switching angles for PWM VSI inverter to eliminate low order voltage harmonic [10] and to optimize dc-link current harmonics [11]. The application of numerous algorithms are proposed for SHE in the literature: Imperial Colonial Algorithm (ICA) [12], Genetic Algorithm [13], Ant Colony Algorithm [14], bee optimization technique (BA) [15], Bacterial Foraging Algorithm [16], Firefly Algorithm (FA) [17], Shuffled Frog Leaping (SFL) algorithm [18], Backtracking Search Algorithm (BSA) and Differential Search Algorithm (DSA) [9], Whale Optimization Algorithm (WOA) [19]. The use of the Grasshopper Optimization Algorithm (GOA) for SHE has not been studied so far.

The GOA is an algorithm recently developed and introduced by Saremi et al. [20] in 2017. In recent two years, the GOA gained great attention in many research fields due to its high efficiency of solving a different kind of optimization problems. It was tested for constrained and unconstrained test functions with promising results [21]. The GOA was proposed for solving multi-objective optimization problems [22] modified by the application of Opposition-Based Learning (OBL) [23]. Modifications of GOA to improve its performance are has been developed and studied: Adaptive GOA (AGOA), Grey Wolf Optimizer (GWO) and Natural Selection (NS) [24], Gaussian mutation, and Leavy- flight strategy [25].

The efficiency of GOA has been compared with existing evolutionary algorithms utilized for different optimization problems. In [26] GOA adaptation for energy loss reduction and voltage stability factor was proposed and compared with PSO, Gravitational Search Algorithm (GSA), and Artificial Bee Colony (BA) algorithms. In [27], the comparison of GOA with PSO and WOA (Wale Optimization Algorithm) was used to optimize the PI controller parameters in the microgrid. Since the first presentation, GOA has found its implementation in numerous industrial applications such as optimization of the parameters of proton membrane fuel cells (PEMFC) [28], the stability of microgrid applications [29] and energy management [30], medicine [31], the technology of image processing [32], and financial issues [25] as well.

In this paper, the recently developed GOA is applied to eliminate low-order voltage harmonics (5th, 7th, 11th, and 13th) in low-frequency VSI based drive. The hypothesis to prove is that GOA represents a higher probability of convergence than PSO applied for SHE problem with similar computation effort. Results for GOA and modified GOA are compared with PSO. The main criterion of comparison is the probability of convergence. The following modification of GOA are examined: Natural Selection (NS), Adaptive GOA (AGOA), Opposite Based Learning (OBL), and Grey Wolf Optimizer (GWO). Experimental results are presented to validate simulation analysis.

The rapid development of controllers for high and medium power converters provides an opportunity for the application of modulation techniques; a decade ago, they used to be known as difficult to use. This type of modulation is SHE-PWM. When it was invented its applicability was very low and nowadays it competes with the most advanced and popular modulations [33]. Its application is studied for grid connectors [34] and railway vehicles [35] as well. Moreover, the separation of a modulator from the controller brings the possibility of implementation of the SHE-PWM with space vector modulation (SVPWM) [36]. Authors of this paper claim that for railway vehicles the most efficient is hybrid modulation studied in [37] where SHE-PWM and SVPWM are used interchangeably and the choice depends on the operating conditions. This solution is the most reasonable and allows to utilize the advantages of both techniques: dynamics of SVPWM and harmonics control of SHE-PWM.

The attention focused on SHE-PWM stimulates research towards increment of efficiency in the calculation of switching angles. In [38] the comprehensive review of SHE-PWM focused on various aspects, is presented. One of the mentioned aspects is the utilization of optimization-based techniques for solving SHE equations and they were divided into four groups: Genetic Algorithms (GA) Particle Swarm Optimization (PSO) Differential Evolution (DE) and Hybrid. According to the “no free lunch” theorem applied to the bio-inspired optimization algorithms [39], there is the most suitable solver for a specific optimization task. Solving SHE equations developed for voltage source inverter is a task of

variable complexity that depends on assumptions like the number of switching angles, modulation index, dead times between switching, switching frequency, and others. Thus, there is a possibility that for different optimization region different algorithm is most suitable. Thus, every recently developed algorithm should be evaluated towards application for solving SHE-PWM equations. In this paper, the authors present the study for the application of the GOA algorithm. The novelty of this study is proof that there is a range of SHE problems where the GOA algorithm gives a higher possibility of convergence with lower computational effort than widely used and appreciated PSO. Results presented in this paper encourage further research to discover the full potential of the GOA algorithm regarding the presented problem by comparing it with a wider representation of bio-inspired algorithms.

The problem undertaken in the study is considered as a single criteria optimization problem. SHE problem could be considered as a multi-objective optimization problem as each harmonic value as a function of optimization variables could be considered as a separate objective function. However, all considered harmonics in the problem of SHE should be eliminated for the same optimization variables, therefore the desirable optimization solution is a utopian solution from the point of view of the multi-optimization approach [40]. Accordingly, the optimization functions have been aggregated to a single optimization variable by means of the dedicated relationship proposed in the article.

2. VSI Model with SHE Control

2.1. Drive's Parameters

The main goal of this work is to study the convergence of GOA applied for the calculation of switching angles for SHE-PWM for a low-frequency VSI drive with an induction motor. Therefore, to prove the validity of results obtained by the examined algorithm, the VSI drive was modeled in MATLAB/SIMULINK and verified in the laboratory. Parameters of utilized induction motor for experiments are presented in Table 1.

Table 1. Parameters of drive's mode.

Symbol	Parameter	Value
P_n	Rated power	2, 5 kW
I_n	Rated phase current	3.9 A
V_n	Rated voltage rms	230/400 V
-	Winding's connection	star
n_n	Rated rotation speed	1465 rpm
L_s	Stator's leakage inductance	0.0108 H
R_s	Stator's resistance	2.8465 Ω
L_r	Rotor's leakage inductance	0.0106 H
R_r	Rotor's resistance	2.7359 Ω
L_m	Core losses inductance	0.27597 H
R_{m_n}	Core losses resistance	1231 Ω

Figure 1a. illustrates the topology of the VSI utilized for the purpose of this work. Figure 1b shows an equivalent circuit of a single phase of the motor applied in the SIMULINK model. Inverter's transistors were controlled by binary switching function ($SF(\omega t)$) formed by switching angles (α) defined as angular "moments" of transistors state change (Figure 2). Switching angles are delivered by solving equations presented in this section.

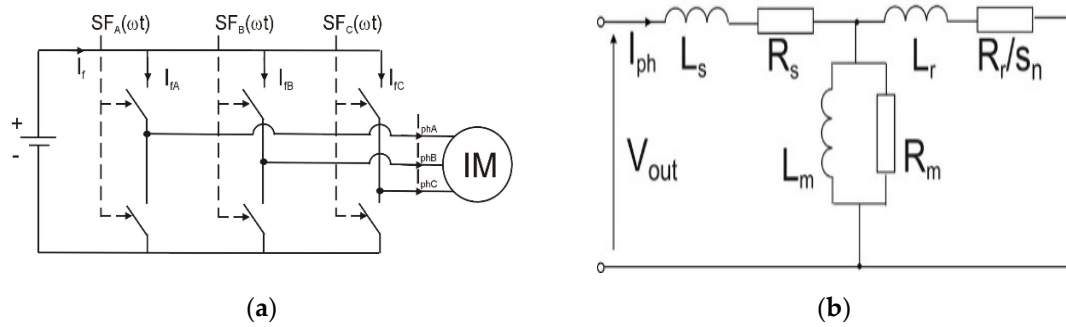


Figure 1. Analytical schema of the considered 3 phase 2-level inverter with load (IM—Model of an induction motor) (a) inverter schema (b) equivalent circuit of one phase of induction motor (sn—Slip for n-th harmonic).

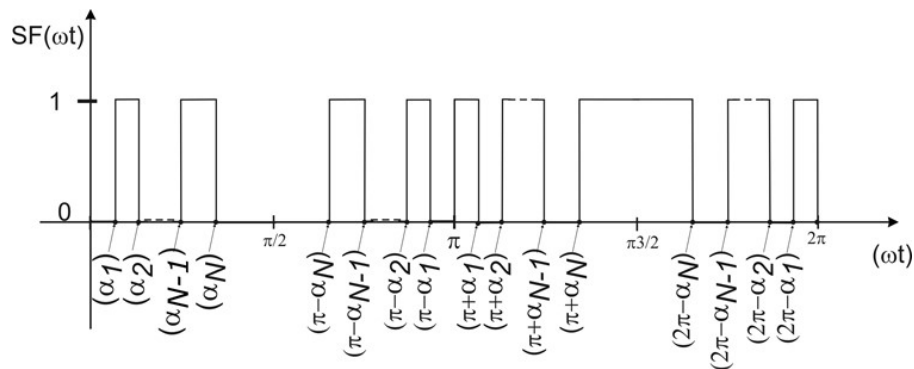


Figure 2. Waveform of switching function SF with quarter-wave symmetry and N switching angles.

2.2. SHE-PWM

In the great number of cases of SHE-PWM application, it is used in electric drives to eliminate low order harmonics, while amplitudes of high order harmonics are reduced by input filters. SHE equations are based on the Fourier series expansion of the inverter output voltage waveform:

$$V(\omega t) = a_0 + \sum_{n=1}^{\infty} [a_n \sin(n\omega t) + b_n \cos(n\omega t)] \tag{1}$$

where ω is an angular frequency of fundamental component, n is a harmonic order, and a_n, b_n are Fourier coefficients. For quarter-wave symmetry, only coefficient a_n for the odd n coefficient represents the non-zero value:

$$a_n = \begin{cases} \frac{4U_{DC}}{n\pi} \left[-1 - 2 \sum_{i=1}^N (-1)^i \cos(n \cdot \alpha_i) \right] & ; \text{ for odd } n \\ 0 & ; \text{ for even } n \end{cases} \tag{2}$$

$$b_n = \begin{cases} 0 & ; \text{ for odd } n \\ 0 & ; \text{ for even } n \end{cases} \tag{3}$$

where U_{DC} is DC-link voltage and n is the number of switching angles per a quarter-period. In this paper, fluctuation and ripples of DC-link voltage were not of concern.

Assuming the odd quarter-wave symmetry of inverter output voltage, triple harmonics are canceled. The symmetry of the system brings cancelation of even harmonics as well. For $n = 5$

switching angles in quarter-period, 5 non-linear equations can be formulated (4) to satisfy fundamental component (V_1) and eliminate 5th, 7th, 11th, and 13th harmonics:

$$\left\{ \begin{array}{l} \frac{4}{\pi}[-1 + 2\cos(\alpha_1) - 2\cos(\alpha_2) + 2\cos(\alpha_3) - \dots \\ \dots 2\cos(\alpha_4) + 2\cos(\alpha_5)] = M1 \\ \frac{4}{5\pi}[-1 + 2\cos(5\alpha_1) - 2\cos(5\alpha_2) + 2\cos(5\alpha_3) - \dots \\ \dots 2\cos(5\alpha_4) + 2\cos(5\alpha_5)] = 0 \\ \frac{4}{7\pi}[-1 + 2\cos(7\alpha_1) - 2\cos(7\alpha_2) + 2\cos(7\alpha_3) - \dots \\ \dots 2\cos(7\alpha_4) + 2\cos(7\alpha_5)] = 0 \\ \frac{4}{11\pi}[-1 + 2\cos(11\alpha_1) - 2\cos(11\alpha_2) + 2\cos(11\alpha_3) - \dots \\ \dots 2\cos(11\alpha_4) + 2\cos(11\alpha_5)] = 0 \\ \frac{4}{13\pi}[-1 + 2\cos(13\alpha_1) - 2\cos(13\alpha_2) + 2\cos(13\alpha_3) - \dots \\ \dots 2\cos(13\alpha_4) + 2\cos(13\alpha_5)] = 0 \end{array} \right. \quad (4)$$

where $M1$ is for modulation index:

$$V_1 = M1 \frac{U_{DC}}{2}; \quad \text{for } M1 \langle 0, \frac{4}{\pi} \rangle \quad (5)$$

In this case the fundamental voltage component (V_1) is defined as the amplitude of phase voltage of the motor in the star connection of the windings. The main goal of this paper is to adopt GOA for solving Equation (4) to determine switching angles for SHE-PWM end examine its convergence.

3. Formulation of The Optimization Problem

To solve SHE Equation (4) using an optimization algorithm, the fitness function must be formulated. For $n = 5$ switching angles and four harmonics eliminated the fitness function is described by following equation with constraints:

$$\begin{aligned} \text{Minimize, } f_{fit}(\alpha_1, \alpha_2, \alpha_3, \alpha_4, \alpha_5) \\ = \sigma_1 \cdot (V_1 - V_1^*)^2 + \sigma_5 \cdot (V_5)^2 + \sigma_7 \cdot (V_7)^2 + \sigma_{11} \cdot (V_{11})^2 + \sigma_{13} \cdot (V_{13})^2 \quad (6) \\ \text{subject to : } 0 < \alpha_1 < \alpha_2 < \alpha_3 < \alpha_4 < \alpha_5 < \frac{\pi}{2} \end{aligned}$$

where: $V_1, V_5, V_7, V_{11}, V_{13}$ are fundamental component and 5th, 7th, 11th and 13th voltage harmonics (p.u.) respectively, σ_x are penalty weights for the optimization process.

Thus, the aim is to apply an optimization algorithm to minimize fitness function (6) to achieve declared fundamental component (V_1^*) and harmonics elimination. The fundamental component is minimized with the highest weigh (penalty value) that equals $\sigma_1 = 100$. Thus, every 1% of difference between an actual value and the desired one will increase fitness function by 100. Harmonics are minimized with penalty weight $\sigma_5 = \sigma_7 = \sigma_{11} = \sigma_{12} = 10$ One of the essential assumptions of every optimization algorithm is the STOP criterion based on the maximum number of iterations and the minimum value of the fitness function. In this paper, the minimum value of the fitness function assumed to be the success is $f_{fit_STOP} = 0.0001$. Regarding the necessity of implementation of dead-times in industrial applications (in this paper $dt = 5 \times 10^{-6}$ s), a lower value of the fitness function will not be recognized as higher quality performance. To prove this statement, sample results obtained by GOA with tolerance 1×10^{-3} (Figure 3a) were compared with the results obtained with tolerance 1×10^{-10} (Figure 3b). Figure 3 shows that decreasing the parameter of tolerance does not guarantee better efficiency of eliminated harmonics, only significantly increases computation time. Thus, tolerance 1×10^{-3} was assumed to be sufficient. More results will be presented in Section 5.

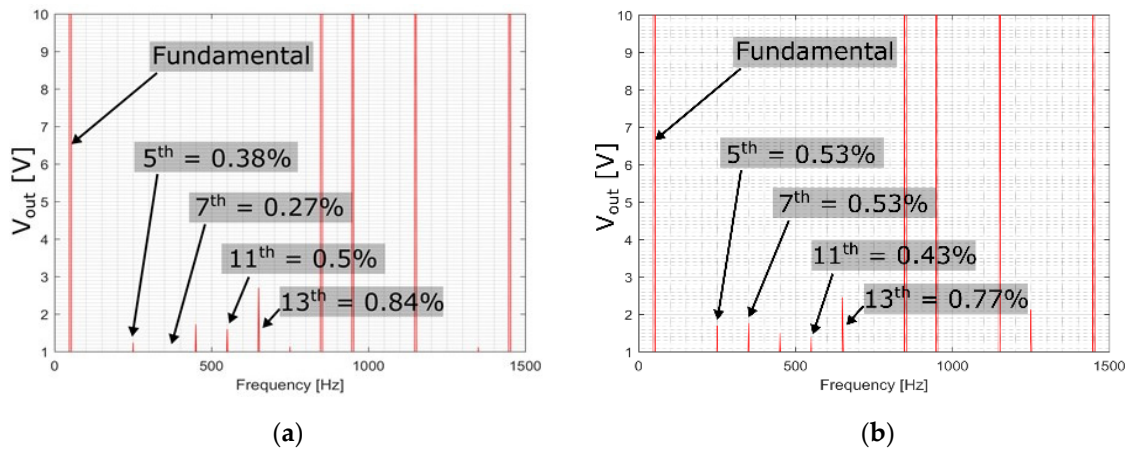


Figure 3. Simulated output voltage spectrum for SHE-SPWM carried out using Grasshopper Optimization Algorithm (GOA) for different tolerance: (a) tolerance $< 1 \times 10^{-4}$; $M1 = 1.0$; $x = (0.1234; 0.4242; 0.5199; 1.2197; 1.2791)$; (b) tolerance $< 1 \times 10^{-10}$; $M1 = 1.0$; $x = (0.1225; 0.4259; 0.5206; 1.2186; 1.2783)$

4. Grasshopper Optimization Algorithm (GOA)

GOA was developed and introduced by Saremi, Mirjalili, and Lewis in [20]. The first proposed application was for structural optimization to find the optimal shape of a three-bar truss, a 52-bar truss, and a Cantilever beam. In this paper, the authors present the application of GOA to solve SHE equations. The proposed algorithm mathematically models the behavior of grasshopper swarm foraging for food to survive. Their individual behavior and social interactions lead the swarm to the optimal solution. The mathematical model of grasshopper behavior is based on a formula for the position of each grasshopper described by the following equation:

$$X_i = S_i + G_i + A_i \tag{7}$$

where X_i is the position of the i -th grasshopper, S_i is the social interaction between agents in the swarm, G_i is the gravity force acting on the i -th grasshopper, and A_i models the wind effect. However, due to specifics of the problems analyzed in this work effect of gravity and wind were omitted. Thus, only social interactions were taken into account.

$$S_i = \sum_{\substack{j=1 \\ j \neq i}}^{Np} s(d_{ij}^*) \cdot \vec{d}_{ij} \tag{8}$$

where d_{ij}^* is the normalized distance between the i -th and j -th grasshopper, $s(d_{ij}^*)$ is the function of social forces and \vec{d}_{ij} is an unitary vector from i -th to j -th grasshopper.

If absolute value of the distance between the i -th and j -th agent is formulated as:

$$d_{ij} = |x_i - x_j| \tag{9}$$

thus, the normalized value is defined as

$$d_{ij}^* = 2 + \text{rem}(d_{ij}, 2) \tag{10}$$

where $\text{rem}(d_{ij}, 2)$ is the remainder after division of d_{ij} by 2. Distance normalization allows for the value of the distance to be kept close to the value of 2 what gives the best effect with the s -function. Unitary vector \vec{d}_{ij} is defined with the following correlation:

$$\begin{cases} \vec{d}_{ij} = 1; \text{ for } x_i - x_j > 0 \\ \vec{d}_{ij} = -1; \text{ for } x_i - x_j \leq 0 \end{cases} \quad (11)$$

Thus, \vec{d}_{ij} can be defined by the following formula:

$$\vec{d}_{ij} = \frac{x_i - x_j}{|x_i - x_j|} \quad (12)$$

A characteristic feature of GOA is a comfort zone shrinking with the iteration number. The Comfort zone is the circle around the best agent. Inside the comfort zone, other agents are being repulsed from the leader and outside the comfort zone, they are being attracted to it. This behavior keeps a balance between exploration and exploitation. The decreasing coefficient c models variation of the comfort zone by changing value typically from 1 to some small number. Regarding the above considerations, Equation (7) for the d -dimensional problem can be expanded as follows:

$$X_i^d = c \left(\sum_{\substack{j=1 \\ j \neq i}}^{Np} c \cdot \frac{ub^d - lb^d}{2} s(d_{ij}^{d*}) \frac{x_i^d - x_j^d}{|x_i^d - x_j^d|} \right) + Gbest^d \quad (13)$$

where ub^d is for upper bound of the d -th dimension, lb^d is for lower bound of the d -th dimension, $Gbest^d$ is for the global best result in the d -th dimension, s is for s -Function which describes the strength of the interaction between agents and is formulated with the following formula:

$$s(d_{ij}^{d*}) = F \cdot e^{(-\frac{d_{ij}^*}{L})} - e^{(-d_{ij}^*)} \quad (14)$$

where F and L are coefficients with suggested values 0.5 and 1.5 respectively. Variation of these coefficients will be analyzed in further sections, regarding its influence on the probability of convergence of the algorithm.

Equation (13) reveals the most significant rule of GOA. The position of agents in every iteration is determined with respect to the position of all other agents in the swarm. For instance, in the PSO algorithm position of agents is determined regarding only two vectors: personal best and global best position. That is the reason why GOA requires a lower population to keep the same computational effort. Moreover, an increment of the swarm population may result in lower convergence.

To apply the GOA algorithm for solving SHE Equation (4) the X_i^d must be correlated with the i -th vector of switching angles $[\alpha_1 \alpha_2 \alpha_3 \alpha_4 \alpha_5]_i$. Thus, in this case, the problem is 5 dimensional. In the following subsections, the modifications of GOA are proposed and tested in section V.

4.1. GOA with GWO Module

Grey Wolf Optimizer is a meta-heuristic algorithm inspired by the behavior of grey wolves and mathematically described by Mirjalili et al. in [41]. The GWO is well studied and can be treated as an independent algorithm. However, its main feature can be implemented in other algorithms. The specifics of the GWO is based on the determination of the three best global solutions called alpha, beta, and gamma. Positions of all particles in the swarm will be updated with respect to the position of

the three best global T_a, T_b, T_c . Thus, to combine GOA and GWO, formula (13) will be modified to the following form [24]:

$$X_i^d = c \left(\sum_{\substack{j=1 \\ j \neq i}}^{Np} c \cdot \frac{ub^d - lb^d}{2} s(d_{ij}^{d*}) \frac{x_i^d - x_j^d}{|x_i^d - x_j^d|} \right) + \frac{T_A^d + T_B^d + T_C^d}{3} \quad (15)$$

4.2. GOA with NS Module

The theory of Natural Selection is based on the random elimination of agents from the swarm with a certain probability P with respect to their fitness value. The better result has a higher chance to survive. Thus, NS requires a classification of the agents then the algorithm calculates P for each agent. To adopt NS for the SHE problem the following formula for P for the i -th agent was developed:

$$P_i = P_{min} + \left[(P_{max} - P_{min}) \cdot \left(\frac{f_{fit_i}}{f_{fit_swarm}} \right) \right] \quad (16)$$

where P_{min} is the minimum assumed probability of survival assigned for the weakest agent; P_{max} is the maximum assumed probability of survival assigned for the best agent; f_{fit_i} is the fitness of the i -th agent; f_{fit_swarm} is the mean value of fitness functions of all agents in the swarm.

The roulette is performed for every single agent regarding its probability of survival. The eliminated agents are replaced by new random solutions.

4.3. Adaptive GOA

Adaptive Grasshopper Optimization Algorithm (AGOA) is based on a dynamic adaptation of the c coefficient regarding the Evolutionary Rate (ER) of the swarm of grasshoppers. ER is defined as the ratio between the number of agents whose fitness was improved in the previous iteration to the total number of agents in the swarm Np . Thus, c for AGOA is defined by the following formula:

$$c(ite) = \left(c_{max} - ite \frac{c_{max} - c_{min}}{t_{max}} \right) F_{ER}(ite) \quad (17)$$

where $F_{ER}(ite)$ is the dynamic adjustment function defined by the following correlation:

$$F_{ER}(ite + 1) = \begin{cases} \frac{F_{ER}(ite)}{F_0}; & \text{for } ER < 15\% \\ F_{ER}(ite); & \text{for } ER \in (15\%; 30\%) \\ F_{ER}(ite) \cdot F_0; & \text{for } ER > 30\% \end{cases} \quad (18)$$

where F_0 is a constant larger than 1. Thus, AGOA presents a dynamic change of comfort zone with a decreasing trend.

4.4. GOA with OBL Module

Opposite Based Learning is a technique of swarm algorithms modification based on the statement that the opposite solution to the developed one might bring better result. Thus, every solution (agent) should be reversed and its fitness should be evaluated. If the fitness of the reversed solution is better than the original, the agent will be replaced. Opposite value \ddot{X}_i^d can be calculated as follows:

$$\ddot{X}_i^d = ub^d + lb^d - X_i^d; \quad (19)$$

for $i = 1, 2, \dots, Np; d = 1, 2, \dots, N$

However, the application of this technique to SHE brings issues regarding the feasibility of calculated solutions. As switching angles are restricted to be sorted according to their feasibility, Equation (19) will reverse their order and make them not feasible. To implement OBL to solve the SHE problem opposite solution \ddot{X}_i^d must be reordered to respect restriction: $0 < \alpha_1 < \alpha_2 < \alpha_3 < \alpha_4 < \alpha_5 < \frac{\pi}{2}$.

5. Simulation Tests and Comparative Study

In this section, a simulation analysis of GOA algorithm performance is presented. Moreover, a comparative study between GOA and modified GOA (NS, AGOA, GWO, and OBL) is carried out. The optimization process has been carried out with the following assumptions:

- STOP criterion of the optimization process is obtained when reaching the assumed maximum number of iterations or the value of the fitness function is below the assumed tolerance 1×10^{-4}
- Every modification module is tested separately. The combination of all modules in one algorithm is not tested. The reason is an increment of computation effort for multi-module algorithm what makes it difficult to compare with single module modifications,
- Swarm population (Np) and maximum number of iterations (max_ite) for comparative study is established regarding similar computational effort (elapsed time of optimization) for compared algorithms.

Figure 4 shows the flow chart of the developed GOA algorithm for SHE with marked modification modules. However, as was mentioned above, only one module is active at the time.

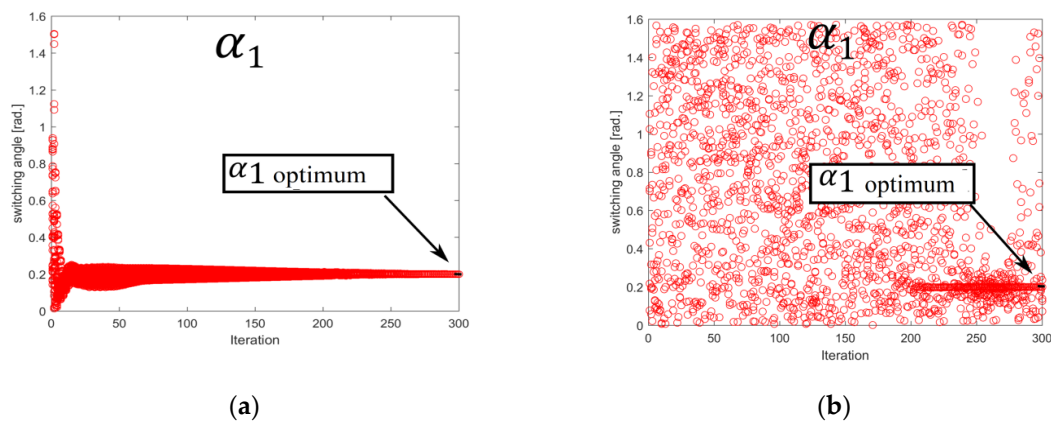


Figure 4. The trajectory of particles in the swarm searching for optimal switching angle α_1 with (a) GOA (b) Particle Swarm Optimization (PSO).

5.1. Comparison between GOA and PSO

The comparative study between GOA and PSO was carried out for $n = 5$ switching angles in a quarter-period, modulation index $M1 = 0.9$, and fundamental frequency $f_f = 50$ Hz what gives 550 Hz switching frequency. In this work 5th, 7th, 11th, and 13th harmonics are eliminated permanently. Figure 5 presents the trajectories of particles during the optimization process with GOA and PSO algorithms, respectively. The GOA algorithm is characterized by a short time of exploration and a long period of exploitation while the PSO algorithm provides a very high intensity of exploration. Figure 6 shows that PSO needs a higher number of iterations to converge comparing with GOA and its modifications.

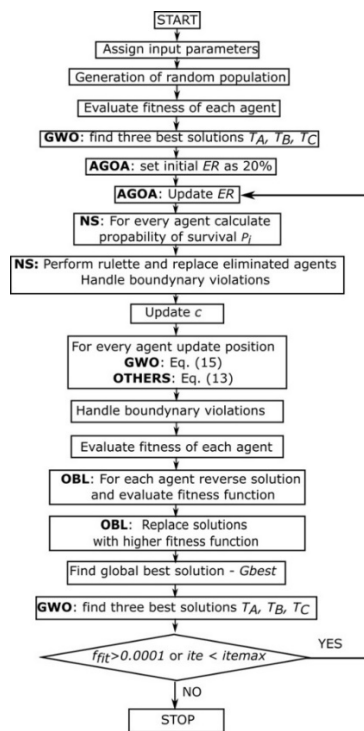


Figure 5. Flow chart of the GOA algorithm with proposed modification.

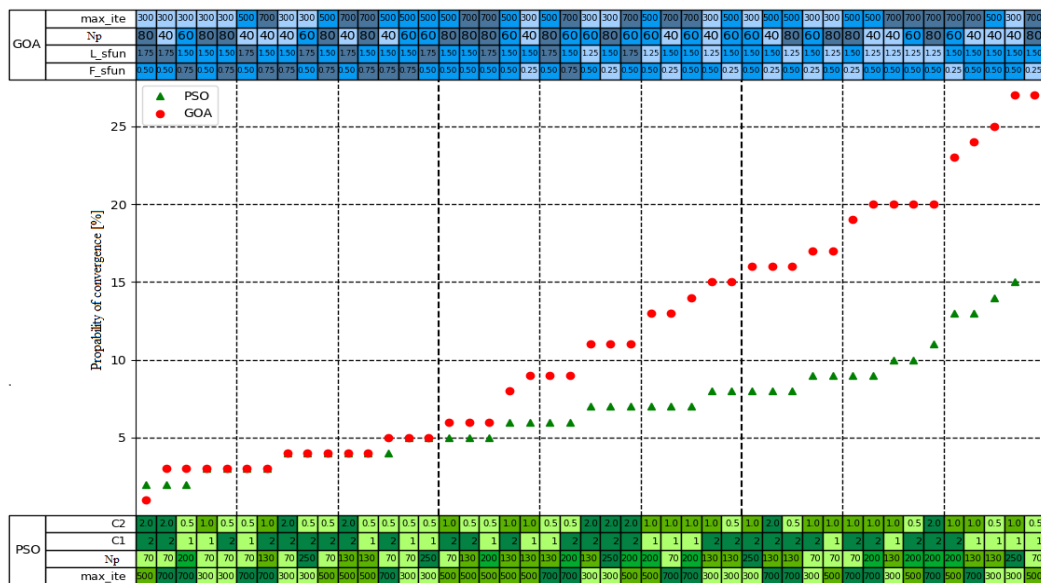


Figure 6. Comparison between PSO and GOA convergence for different values of coefficients.

In the following part of this section, the convergence of GOA and PSO has been compared. The various combinations of parameters were tested. For every set of both GOA and PSO, 100 runs were calculated. For each series of runs, the number of runs that reaches f_{fit} below 1×10^{-4} was recorded as the success. The variation of the following parameters was studied: maximum number of iterations (max_ite), size of the population (Np), PSO parameters C1 and C2, and GOA parameters used in s-function (L and F). Thus, all results have been presented in Figure 6 where the probability of convergence is compared. The value of population size for PSO and GOA was adjusted to keep similar computation times for both.

The best performance of GOA was recorded for settings: $Np = 40$, $max_ite = 300$, $L = 1.5$ and $F = 0.5$. For the aforementioned setting, GOA achieved 27% convergence (time of computation 101 s). The PSO

achieved the best performance for: $N_p = 250$, $max_ite = 300$, $C1 = 1$ and $C2 = 0.5$. Thus, GOA presents better performance than PSO regarding higher convergence for lower population size. Results presented in Figure 6 proves that for the SHE problem the GOA presents a significantly higher probability of convergence than the PSO algorithm. The most interesting result was achieved by using the GOA algorithm for population 40 and 300 iterations (the second-highest for this algorithm) where the probability of convergence was 28%. This result proves that the GOA algorithm can be very efficient for low population set up which reduces its computational effort. The highest recorded probability of convergence of PSO during the experiment was 15% (time of computation 260 s). The GOA algorithm gives a better result faster. The computation effort is extremely significant during the application of the optimization task for the task. In this paper, coefficients of the compared algorithm were selected in such a way to keep comparable computation time. The parameters which are affecting computation time are population size N_p and the maximum number of iteration max_ite . Results presented in Figure 6 can be divided into 9 SETS regarding N_p and max_ite . Table 2 presents computation time for the PSO and GOA performed on a computer with processor *Intel Core i7-8557U*. Results from Table 2 are presented in Figure 7. The parameters N_p and max_ite were selected to keep similar computation time for GOA and PSO for one SET. The GOA in every iteration calculates the position of every agent (grasshopper) related to every agent in the swarm, PSO calculates the only position of the agent related to the position of the pest particle. That is why GOA needs higher computational effort than PSO for the same N_p . Thus, to make it comparable the N_p for GOA was reduced in every SET.

Table 2. Sets of coefficients with computation time (100 runs).

No.	PSO			GOA		
	Max_Ite	Np	Time [s]	Max_Ite	Np	Time [s]
SET 1	300	70	99	300	40	101
SET 2	300	130	169	300	60	163
SET 3	300	250	260	300	80	261
SET 4	500	70	165	500	40	152
SET 5	500	130	310	500	60	277
SET 6	500	250	470	500	80	438
SET 7	700	70	245	700	40	264
SET 8	700	130	412	700	60	385
SET 9	700	250	637	700	80	687

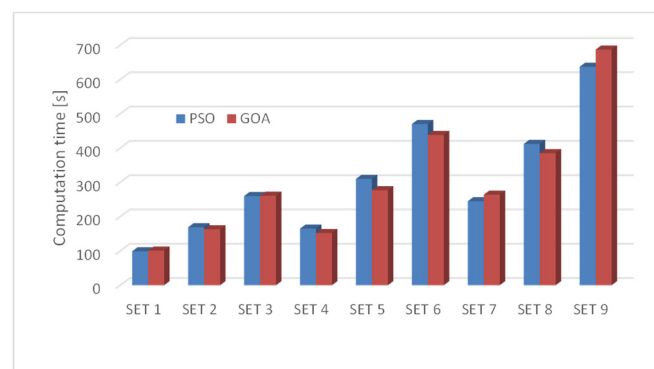


Figure 7. Computation time for different sets of coefficients.

Figure 8 shows the switching angles calculated by PSO and not modified GOA as the function of modulation index M1.

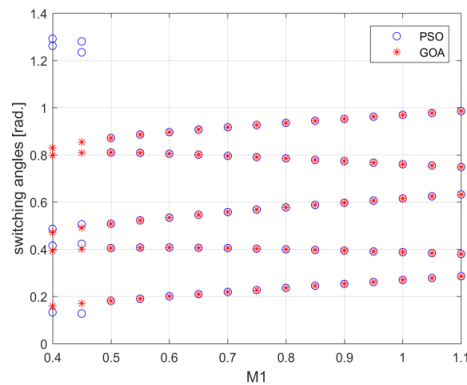


Figure 8. Switching angles as the function of modulation index $M1$ for SHE-PWM calculated using PSO and GOA.

5.2. Comparative Study between PSO, GOA, and Modified GOA

In this subsection, the convergence of GOA with modifications and PSO algorithms has been carried out. Assumptions from section *V A* and Table 3 are valid in this section. However, the comparison has been conducted for a wider range of modulation index $M1 = 0.4 \div 1.1$.

Table 3. Parameters for all analysis.

Algorithm	Coefficients	Value
GOA	c_{min}	1×10^{-6}
	c_{max}	1
GOA + NS	P_{min}	0.3
	P_{max}	0.95
AGOA	F_0	1.05
PSO	$C1$	2
	$C2$	2
	w_{min}	1×10^{-3}
	w_{max}	1

The comparative study reveals that the most efficient with the highest probability of convergence is the GOA algorithm modified by adding the OBL module (Figure 9). The convergence of the studied algorithm was decreasing with an increase of $M1$ because higher modulation index requires smaller spaces between switching angles and reduce the feasibility of developed solutions. For $M1$ in the range from 0.7 to 0.8 modification based on NS presented very good performance as well. Figure 10 presents the examination of fitness value (f_{fit}) as the function of the iteration number. The conclusion is that GOA-based algorithms present significantly faster convergence than PSO.

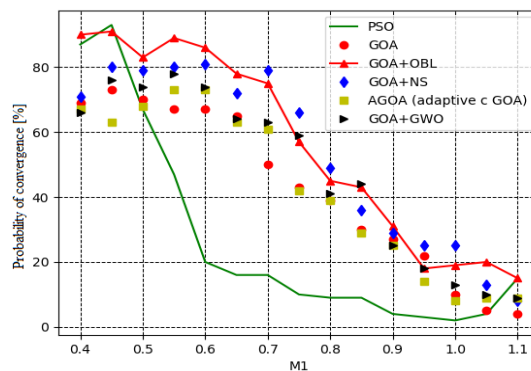


Figure 9. Comparison of the probability of convergence between PSO, GOA, and modified GOA algorithms.

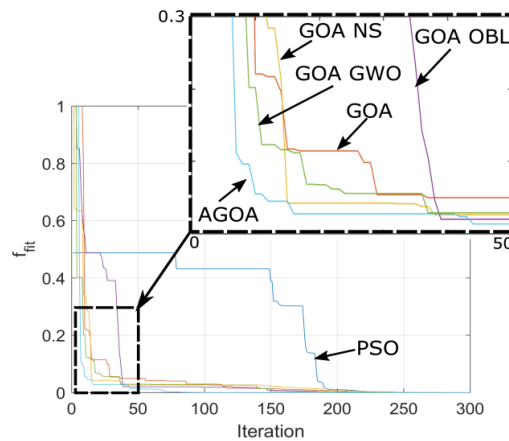


Figure 10. Fitness value versus iteration number for examined algorithms.

6. Experimental Results

The applied GOA algorithm has been experimentally verified. Switching angles calculated by the GOA algorithm were implemented into the laboratory stand (Figure 11) developed according to Figure 1. Parameters of the induction motor applied in the laboratory stand are presented in Table 1. The inverter control by switching angles input was provided by DSpace card 1104. Switching angles were applied as the look-up table for off-line control. Verification was conducted for two operating points with the same fundamental frequency $f_f = 50$ Hz, and different $M1 = 0.9$ and 1.0 , respectively.

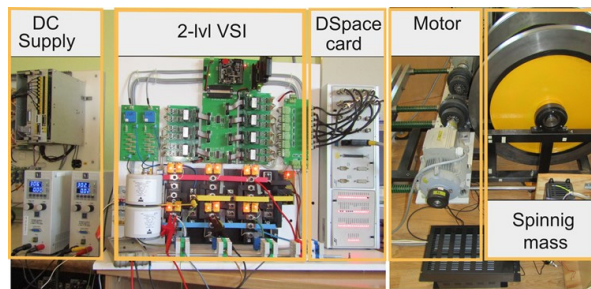


Figure 11. Laboratory stands for experimental tests.

In Figures 12 and 13 it can be noticed that amplitudes of 5th, 7th, 11th, and 13th harmonics in the output voltage have been eliminated and the GOA algorithm has successfully minimized the goal function.

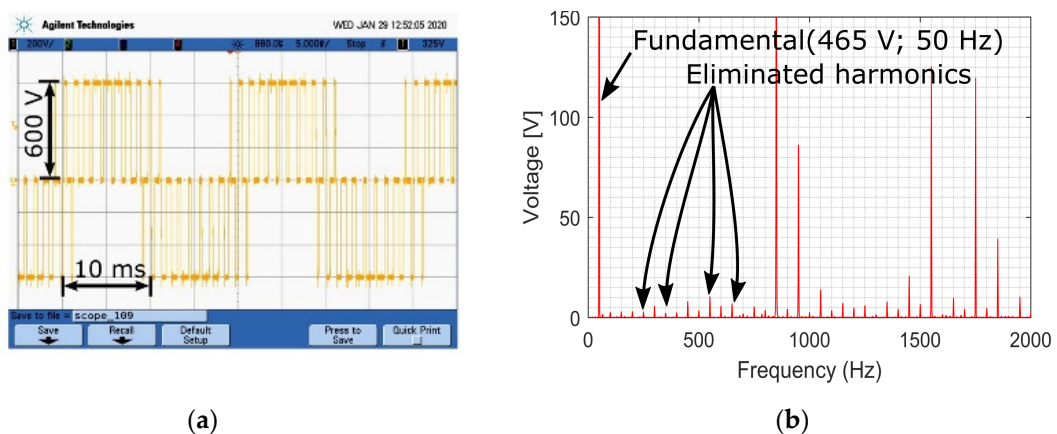


Figure 12. Experimental results for inverter's phase to phase output voltage for $M1 = 0.9$ (a) waveform oscillogram (b) spectrum.

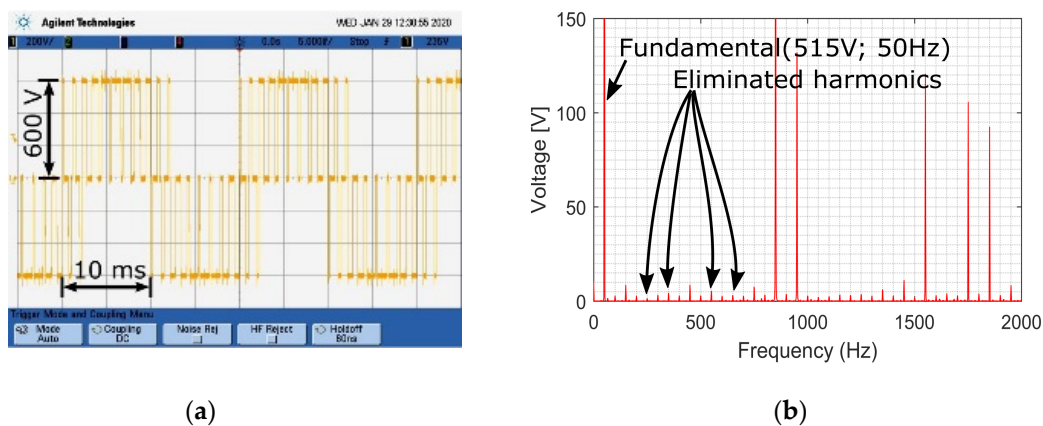


Figure 13. Experimental results for inverter's output phase to phase voltage for $M1 = 1.0$ (a) waveform oscillogram (b) spectrum.

7. Conclusions

In this paper, the authors investigated a novel application of a recently developed GOA algorithm, for the calculation of switching angles in SHE-PWM inverter modulation. The main goal of this paper was to examine the probability of convergence introduced by GOA applied for solving the SHE problem. Modifications of the GOA algorithm have been implemented and compared with the PSO algorithm. The GOA algorithm is based on the behavior of a swarm of grasshoppers and the most characteristic feature is that the movement of agents depends not only on the position related to the position of the best agent (best global solution) but it depends on the position related to the other agents as well. Thus, the results prove that the GOA algorithm requires a lower population size to converge with computation effort similar to PSO. The most interesting outcome of this study is that the GOA algorithm with OBL elements proves its superiority over the PSO algorithm regarding the probability of convergence for similar computational effort (lower population of particles). The second most efficient combination was the GOA algorithm with NS modification. GOA presents the highest advantage over PSO in the range of modulation index from 0.5 to 1.0. In this range, the convergence of PSO was dramatically reduced (below 5% in the worst case), and meanwhile, the probability of convergence of GOA was between 20 and 80%. The performed measurement experiments proved that the SHE-PWM waveform optimized by the GOA algorithm provided elimination of the chosen harmonics in the inverter's output voltage. In the nearest future, authors will focus their attention on the application of the GOA algorithm for optimization of waveforms generated by multilevel inverters and its applicability in traction drive solutions.

Author Contributions: M.S.: Concept and methodology of the research, development of software and application of algorithms. Formulation of conclusions. W.J.: Laboratory measurements and presentation of results. A.S.: Research supervision and text formatting. All authors have read and agreed to the published version of the manuscript.

Funding: This research received no external funding.

Conflicts of Interest: The authors declare no conflict of interest.

References

1. Lou, H.; Mao, C.; Lu, J.; Wang, D.; Lee, W.J. Pulse width modulation AC/DC converters with line current harmonics minimisation and high power factor using hybrid particle swarm optimisation. *IET Power Electron.* **2009**. [[CrossRef](#)]
2. Sharifzadeh, M.; Vahedi, H.; Portillo, R.; Khenar, M.; Sheikholeslami, A.; Franquelo, L.G.; Al-Haddad, K. Hybrid SHM-SHE Pulse-Amplitude Modulation for High-Power Four-Leg Inverter. *IEEE Trans. Ind. Electron.* **2016**, *63*, 7234–7242. [[CrossRef](#)]
3. Turnbull, F.G. Selected Harmonic Reduction in Static D-C—A-C Inverters. *IEEE Trans. Commun. Electron.* **1964**, *83*, 374–378. [[CrossRef](#)]

4. Patel, H.S.; Hoft, R.G. Generalized Techniques of Harmonic Elimination and Voltage Control in Thyristor Inverters: Part I—Harmonic Elimination. *IEEE Trans. Ind. Appl.* **1973**, *IA-9*, 310–317. [[CrossRef](#)]
5. Patel, H.S.; Hoft, R.G. Generalized techniques of harmonic elimination and voltage control in thyristor inverters: Part II—voltage control techniques. *Technology* **1974**, *IA-10*, 666–673. [[CrossRef](#)]
6. Sharifzadeh, M.; Vahedi, H.; Portillo, R.; Franquelo, L.G.; Al-Haddad, K. Selective Harmonic Mitigation Based Self-Elimination of Triplen Harmonics for Single-Phase Five-Level Inverters. *IEEE Trans. Power Electron.* **2018**, *34*, 86–96. [[CrossRef](#)]
7. Chiasson, J.N.; Member, S.; Tolbert, L.M.; Mckenzie, K.J.; Member, S.; Du, Z. Elimination Problem. *IEEE Trans. Power Electron.* **2004**, *19*, 491–499. [[CrossRef](#)]
8. Yang, K.; Zhang, Q.; Yuan, R.; Yu, W.; Wang, J. Harmonic elimination for multilevel converter with Groebner bases and symmetric polynomials. In Proceedings of the 2015 IEEE Energy Conversion Congress and Exposition (ECCE), Montreal, QC, Canada, 20–24 September 2015; Volume 31, pp. 689–694. [[CrossRef](#)]
9. Kundu, S.; Burman, A.D.; Giri, S.K.; Mukherjee, S.; Banerjee, S. Comparative study between different optimisation techniques for finding precise switching angle for SHE-PWM of three-phase seven-level cascaded H-bridge inverter. *IET Power Electron.* **2018**, *11*, 600–609. [[CrossRef](#)]
10. Ray, R.N.; Chatterjee, D.; Goswami, S.K. An application of PSO technique for harmonic elimination in a PWM inverter. *Appl. Soft Comput.* **2009**, *9*, 1315–1320. [[CrossRef](#)]
11. Steczek, M.; Chudzik, P.; Szelag, A. Combination of SHE and SHM—PWM techniques for VSI DC-link current harmonics control in railway applications. *IEEE Trans. Ind. Electron.* **2017**. [[CrossRef](#)]
12. Etesami, M.H.; Vilathgamuwa, D.M.; Ghasemi, N.; Jovanovic, D.P. Enhanced Metaheuristic Methods for Selective Harmonic Elimination Technique. *IEEE Trans. Ind. Inform.* **2018**, *14*, 5210–5220. [[CrossRef](#)]
13. Dahidah, M.S.A.; Agelidis, V.G. Selective harmonic elimination PWM control for cascaded multilevel voltage source converters: A generalized formula. *IEEE Trans. Power Electron.* **2008**, *23*, 1620–1630. [[CrossRef](#)]
14. Sundareswaran, K.; Jayant, K.; Shanavas, T.N. Inverter harmonic elimination through a colony of continuously exploring ants. *IEEE Trans. Ind. Electron.* **2007**, *54*, 2558–2565. [[CrossRef](#)]
15. Kavousi, A.; Vahidi, B.; Salehi, R.; Bakhshizadeh, M.K.; Farokhnia, N.; Fathi, S.H. Application of the bee algorithm for selective harmonic elimination strategy in multilevel inverters. *IEEE Trans. Power Electron.* **2012**, *27*, 1689–1696. [[CrossRef](#)]
16. Sudhakar Babu, T.; Priya, K.; Maheswaran, D.; Sathish Kumar, K.; Rajasekar, N. Selective voltage harmonic elimination in PWM inverter using bacterial foraging algorithm. *Swarm Evol. Comput.* **2015**, *20*, 74–81. [[CrossRef](#)]
17. Gnana Sundari, M.; Rajaram, M.; Balaraman, S. Application of improved firefly algorithm for programmed PWM in multilevel inverter with adjustable DC sources. *Appl. Soft Comput.* **2016**, *41*, 169–179. [[CrossRef](#)]
18. Lou, H.; Mao, C.; Wang, D.; Lu, J.; Wang, L. Fundamental modulation strategy with selective harmonic elimination for multilevel inverters. *IET Power Electron.* **2014**, *7*, 2173–2181. [[CrossRef](#)]
19. Kar, P.K.; Priyadarshi, A.; Karanki, S.B. Selective harmonics elimination using whale optimisation algorithm for a single-phase-modified source switched multilevel inverter. *IET Power Electron.* **2019**, *12*, 1952–1963. [[CrossRef](#)]
20. Saremi, S.; Mirjalili, S.; Lewis, A. Grasshopper Optimisation Algorithm: Theory and application. *Adv. Eng. Softw.* **2017**, *105*, 30–47. [[CrossRef](#)]
21. Neve, A.G.; Kakandikar, G.M.; Kulkarni, O. Application of Grasshopper Optimization Algorithm for Constrained and Unconstrained Test Functions. *Int. J. Swarm Intell. Evol. Comput.* **2017**, *6*. [[CrossRef](#)]
22. Mirjalili, S.Z.; Mirjalili, S.; Saremi, S.; Faris, H.; Aljarah, I. Grasshopper optimization algorithm for multi-objective optimization problems. *Appl. Intell.* **2018**, *48*, 805–820. [[CrossRef](#)]
23. Ewees, A.A.; Abd Elaziz, M.; Houssein, E.H. Improved grasshopper optimization algorithm using opposition-based learning. *Expert Syst. Appl.* **2018**, *112*, 156–172. [[CrossRef](#)]
24. Wu, J.; Wang, H.; Li, N.; Yao, P.; Huang, Y.; Su, Z.; Yu, Y. Distributed trajectory optimization for multiple solar-powered UAVs target tracking in urban environment by Adaptive Grasshopper Optimization Algorithm. *Aerosp. Sci. Technol.* **2017**, *70*, 497–510. [[CrossRef](#)]
25. Luo, J.; Chen, H.; Xu, Y.; Huang, H.; Zhao, X. An improved grasshopper optimization algorithm with application to financial stress prediction. *Appl. Math. Model.* **2018**, *64*, 654–668. [[CrossRef](#)]

26. Sultana, U.; Khairuddin, A.B.; Sultana, B.; Rasheed, N.; Hussain, S.; Riaz, N. Placement and sizing of multiple distributed generation and battery swapping stations using grasshopper optimizer algorithm. *Energy* **2018**, *165*, 408–421. [[CrossRef](#)]
27. Jumani, T.A.; Mustafa, M.W.; Rasid, M.M.; Mirjat, N.H.; Leghari, Z.H.; Salman Saeed, M. Optimal voltage and frequency control of an islanded microgrid using grasshopper optimization algorithm. *Energies* **2018**, *11*, 3191. [[CrossRef](#)]
28. El-Fergany, A.A. Electrical characterisation of proton exchange membrane fuel cells stack using grasshopper optimizer. *IET Renew. Power Gener.* **2018**, *12*, 9–17. [[CrossRef](#)]
29. Barik, A.K.; Das, D.C. Expeditious frequency control of solar photovoltaic/biogas/biodiesel generator based isolated renewable microgrid using grasshopper optimisation algorithm. *IET Renew. Power Gener.* **2018**, *12*, 1659–1667. [[CrossRef](#)]
30. Liu, J.; Wang, A.; Qu, Y.; Wang, W. Coordinated Operation of Multi-Integrated Energy System Based on Linear Weighted Sum and Grasshopper Optimization Algorithm. *IEEE Access* **2018**, *6*, 42186–42195. [[CrossRef](#)]
31. Tumuluru, P.; Ravi, B. GOA-based DBN: Grasshopper optimization algorithm-based deep belief neural networks for cancer classification. *Int. J. Appl. Eng. Res.* **2017**, *12*, 14218–14231.
32. Liang, H.; Jia, H.; Xing, Z.; Ma, J.B.; Peng, X. Modified Grasshopper Algorithm-Based Multilevel Thresholding for Color Image Segmentation. *IEEE Access* **2019**, *7*, 11258–11295. [[CrossRef](#)]
33. Leon, J.I.; Kouros, S.; Franquelo, L.G.; Rodriguez, J.; Wu, B. The Essential Role and the Continuous Evolution of Modulation Techniques for Voltage-Source Inverters in the Past, Present, and Future Power Electronics. *IEEE Trans. Ind. Electron.* **2016**, *63*, 2688–2701. [[CrossRef](#)]
34. Napoles, J.; Leon, J.I.; Portillo, R.; Franquelo, L.G.; Aguirre, M.A. Selective harmonic mitigation technique for high-power converters. *IEEE Trans. Ind. Electron.* **2010**, *57*, 2315–2323. [[CrossRef](#)]
35. Youssef, M.Z.; Woronowicz, K.; Aditya, K.; Azeez, N.A.; Williamson, S.S. Design and development of an efficient multilevel DC/AC traction inverter for railway transportation electrification. *IEEE Trans. Power Electron.* **2016**, *31*, 3036–3042. [[CrossRef](#)]
36. Wang, Y.; Wen, X.; Guo, X.; Zhao, F.; Cong, W. Vector control of induction motor based on selective harmonic elimination PWM in medium voltage high power propulsion system. In Proceedings of the 2011 International Conference on Electric Information and Control Engineering, Wuhan, China, 15–17 April 2011; pp. 6351–6354. [[CrossRef](#)]
37. Zhang, Y.; Zhao, Z.; Zhu, J. A hybrid PWM applied to high-power three-level inverter-fed induction-motor drives. *IEEE Trans. Ind. Electron.* **2011**, *58*, 3409–3420. [[CrossRef](#)]
38. Dahidah, M.S.A.; Konstantinou, G.; Agelidis, V.G. A Review of Multilevel Selective Harmonic Elimination PWM: Formulations, Solving Algorithms, Implementation and Applications. *IEEE Trans. Power Electron.* **2015**, *30*, 4091–4106. [[CrossRef](#)]
39. Orosz, T.; Rassölkin, A.; Kallaste, A.; Arsénio, P.; Pánek, D.; Kaska, J.; Karban, P. Robust Design Optimization and Emerging Technologies for Electrical Machines: Challenges and Open Problems. *Appl. Sci.* **2020**, *10*, 6653. [[CrossRef](#)]
40. Marler, R.T.; Arora, J.S. Survey of multi-objective optimization methods for engineering. *Struct. Multidiscip. Optim.* **2004**, *26*, 369–395. [[CrossRef](#)]
41. Mirjalili, S.; Mirjalili, S.M.; Lewis, A. Grey Wolf Optimizer. *Adv. Eng. Softw.* **2014**, *69*, 46–61. [[CrossRef](#)]

Publisher’s Note: MDPI stays neutral with regard to jurisdictional claims in published maps and institutional affiliations.



© 2020 by the authors. Licensee MDPI, Basel, Switzerland. This article is an open access article distributed under the terms and conditions of the Creative Commons Attribution (CC BY) license (<http://creativecommons.org/licenses/by/4.0/>).